Title

Damage-free X-ray spectroscopy characterization of oxide thin films

Authors

Lainé, Antoine
Parmar, Rahul
Amati, Matteo
et al.

Publication Date

2023-10-01

DOI

10.1016/j.apsusc.2023.157335

Peer reviewed

Damage-free X-ray spectroscopy characterization of oxide thin films

Antoine Lainé[1*], Rahul Parmar[2], Matteo Amati[2], Luca Gregoratti[2], Gregory Su[1,3], Ting Xu[1,4,5] and Miquel Salmeron[1,5**]

[1] *Materials Sciences Division, Lawrence Berkeley National Laboratory, Berkeley, California 94720, United States*

[2] *Elettra-Sincrotrone Trieste S.C.p.A. di interesse nazionale, Strada Statale 14 - km 163,5 in AREA Science Park, 34149 Basovizza, Trieste ITALY*

[3] *Advanced Light Source, Lawrence Berkeley National Laboratory, Berkeley, California 94720, United States*

[4] *Department of Chemistry, University of California, Berkeley, California 94720, United States*

[5] *Department of Materials Science and Engineering, University of California, Berkeley, California 94720, United States*

[*] antoinelaine@lbl.gov

[**] mbsalmeron@lbl.gov

Abstract

Thin polymer or oxide films are ubiquitous components in many devices, including membranes for filtration or electrodes in electrochemical energy storage. High energy electron or x-ray probes for microscopy and spectroscopy are useful to characterize and understand these materials. However, irreversible damage by the probe radiation remains a challenge. Here, we show that graphene serves as an x-ray and electron transparent substrate that substantially reduces radiation damage of an oxide thin film. We demonstrate this using highly focused x-ray beams, which show that compared to oxide thin films supported on a substrate, graphene-supported regions show minimal changes in the x-ray spectra as a function of x-ray dose. These results pave the way for the development of experimental setups that allow for long exposure time measurements with limited sample damage and substrate-directed radiation patterning.

1 Introduction

The advent of nanotechnology and miniaturization of many devices require size reduction of the individual material building blocks. Coatings [?], membranes [?] or electrodes [?], that are just several nanometers thick are routinely used. For example, photoresist thin films used for mask lithography in the semiconductor industry are typically tens of nanometers thick [?].

Microscopy and spectroscopy techniques based on high energy electron and x-ray probes are used extensively to characterize the structure and chemical state of materials [?, ?, ?]. An undesirable side effect of these charcterization techniques is the beam-induced modification/damage of the sample [?, ?, ?]. On the other hand, the beam-induced damage is of interest when used for patterning purposes like in electron beam lithography [?]. It is therefore crucial to understand the damage mechanism and its origin. While beam damage can occur in nearly all materials, it is particularly acute in thin films, including adsorbed molecules, organic layers, polymers, oxide films, semiconductor materials, and protective layers.

Radiation damage takes place as the energy of the incident beam is absorbed by the material under study, leading to electronic transitions between occupied and empty electron states, phonon excitations, impact processes, or other processes. Several efforts have already been made to study the cause, mechanisms and impacts of beam damage during irradiation [?, ?]. Thin films are good model systems to study damage with highly surface-sensitive x-ray techniques. Self-assembled monolayers (SAMs) deposited over a metallic substrate exhibit degradation that is highly influenced by the radiation dose [?, ?, ?]. Several procedures are commonly used to avoid such damage, including continuously scanning across the sample surface to change the target spot of the the incident beam, reducing the incident beam flux, and defocusing. These strategies can reduce damage, but do so at the expense of a loss of spatial resolution and signal to noise ratio [?].

Similarities between X-ray and electron beam induced damage of thin polymer films indicate that the nature of the incident radiation does not influence damage as much as the secondary electrons generated in the sample material [?, ?]. It has been shown that the damage observed in supported SAM correlates with the ability of the supporting substrate to provide secondary electrons [?, ?], and this shows the importance of the substrate and its role as a source of secondary electrons. These secondary electrons, with a typical energy ≤ 50 eV, are primarily responsible for the chemical damage generated in the supported material.

Our work aims at providing an in-depth understanding of damage in a sample supported by a substrate of controlled thickness. Our strategy to limit beam damage

is to support the sample on atomically thin graphene to reduce the amount of secondary electrons that enter the sample. High energy spectroscopy characterization requires being able to disentangle beam damage from material evolution that is being probed. As a consequence,knowledge of the sample damage dynamics is particularly important. Such damage dynamics is cumbersome for beam patterning purposes and controlling the nature of the substrate could open new manufacturing opportunities.

2 Material and Methods

2.1 Sample fabrication and characterization

Commercially available SiN_x membranes patterned with an ordered square array of ~ 1 μm diameter holes were coated with Cr (2nm) and Au (20nm). A polymer-free wet transfer technique was used to detach the graphene layer from its copper foil for deposition onto the membrane [**?**]. The graphene-covered membrane was annealed at 300°C under vacuum overnight. Raman spectroscopy was used to characterize the number of graphene layers present (see SI figure S1) [**?**]. An AFM image of the resulting sample (SI figure SI2 (b)) evidences the graphene coverage over the entire membrane. Then, a TiO_2 film $\sim$ 2.5 nm thick (as measured by ellipsometry) was grown on top of the graphene using Plasma Enhanced Atomic Layer Deposition [**?**]. A Transmission Electron Microscopy image (SI figure SI2 (c)) of a region containing a hole highlights the uniform and amorphous structure of the sample. Lab-based XPS of the Ti 2p spectral region (SI figure SI2 (d)) exhibits two peaks around 458 and 463 eV that corresponds to the Ti^{4+} oxidation state characteristic of TiO_2 [**?**, **?**]. X-ray Absorption Spectroscopy experiments (SI figure SI2 (e)) of the Ti L-edge further confirms the amorphous nature of the TiO_2 film as revealed by the t_{2g} peak at 457 eV being significantly smaller than the e_g peak at 459 eV [**?**, **?**].

2.2 X-ray photoelectron spectro-microscopy experiments

X-ray Photoelectron experiments were performed at the ESCA Microscopy beamline at the Elettra synchrotron, which can focus the incident x-ray beam to achieve a spot diameter of $\approx$ 150 nm using zone plates (see Supplementary information S2.1 for details regarding the beamline characteristics). We can estimate the fluence, defined as the amount of photons per unit area illuminating the sample as:

$$a(t) = \frac{\Phi_0 t}{\mathcal{A}}$$

with Φ_0 being the incident flux in photons/s, t the exposure time and $\mathcal{A}$ the exposed area of the sample. The photon density at the sample with the focused beam $\Phi_0/\mathcal{A} \approx 10^{12}$ photons.s^{-1}.μm^{-2}.

For these experiments, the incident photon energy is 650.7 ± 0.1 eV.

3 Results and discussion

3.1 Spatially resolved beam damage

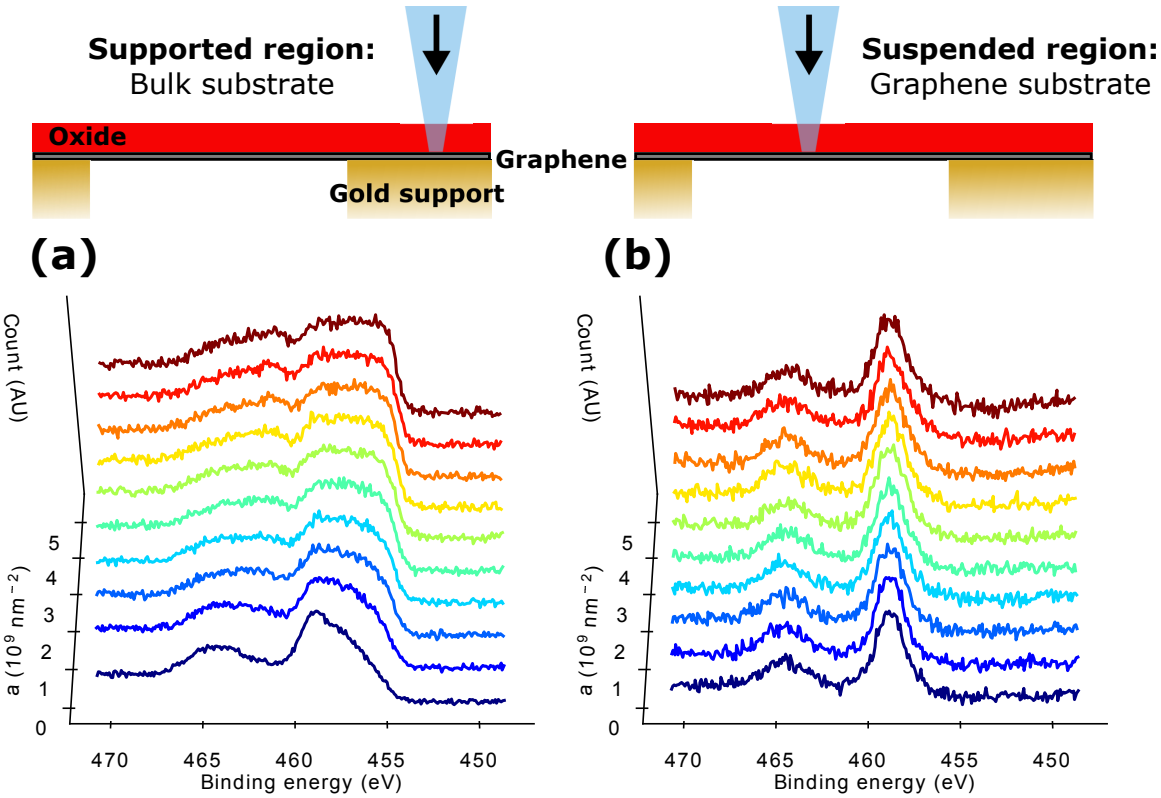

Figure 1: **Spatially resolved beam induced damage for single layer graphene** High resolution Ti 2p spectra (XPS) for increasing fluence values, $a = \Phi_0 t/\mathcal{A}$, for the beam focused over **(a)** supported and **(b)** suspended regions. Insets above each figure display a schematic representation of the beam configuration and subsequent sample exposure.

Figure 1 shows the evolution of the XPS spectra of oxide films for supported and suspended regions as the incident x-ray exposure increases. The oxide film on graphene sample is illuminated from the front side as illustrated in the schematic drawings at the top of figure 1. Multiple XPS spectra were collected over time at the

same position in order to probe damage induced in the material as function of fluence.

The incident x-ray beam is focused to a spot size of $\sim$ 150 nm. As the oxide film deposited on graphene is lying over a perforated substrate with $\sim$ 1 μm holes, we could easily focus the beam over a supported (Figure 1 (a)) or suspended region (Figure 1 (b)).

Figure 1 (a) exhibits the XPS spectra of a supported region of the sample as the fluence increases. We clearly observe a significant change in the spectral response as fluence increases, corresponding to damage. The XPS peaks of Ti^{3+} and Ti^{2+} oxidation states have binding energies shifted by $\Delta BE_{Ti^{3+}} \approx 2$ eV and $\Delta BE_{Ti^{2+}} \approx 4$ eV relative to the Ti^{4+} peak [**?**], indicative of the chemical reduction of the Ti atoms. The damage is attributed to low-energy secondary electrons breaking Ti-O bonds and leading to the creation of oxygen vacancies manifested in the generation of Ti^{3+} and Ti^{2+} species [**?**, **?**]. A similar damage mechanism is observed in a TiO_2 film under Ar^+ ion bombardment [**?**], which also produces O vacancies. Some signs of damage are already apparent for the spectrum acquired at the lowest beam exposure. The minimum achievable fluence $a_{min} \approx 6.10^8$ nm^{-2} is already sufficient to trigger damage in the supported film.

Figure 1 (b) displays the XPS spectral evolution of a graphene-suspended region of the TiO_2 film. In contrast, we do not observe any variation of the XPS spectra as the fluence increases. This observation highlights the significant beam damage mitigation achieved by suspending the film on graphene. The maximum fluence of $a_{max} \approx 6.10^9$ nm^{-2} shows that the critical dose is at least an order of magnitude larger than for a sample supported on a thicker substrate. In addition, we note the absence of any systematic shift of the binding energies revealing the ability of the conducting graphene to avoid charging in the sample.

The 2.5nm-thick TiO_2 film is only slightly larger than the inelastic mean free path of electrons in the material ($\approx$ 1 nm). In this case, no significant damage is observed over our observation time scale as most photo-generated electrons escape the sample after suffering no or only a very few collisions in the sample.

3.2 Source of damaging electrons

From Figure 1 (a) to Figure 1 (b), the substrate thickness was decreased from $\sim$ 100 nm to the 1 atom-thick graphene. As a consequence, the amount of secondary electrons originating from the substrate is significantly decreased. The high transparency of graphene to x-rays and electrons [**?**] leads to a vanishingly small secondary electron

yield, at least one order of magnitude smaller than typical metals [**?**, **?**]. Therefore, a negligible amount of secondary electrons originate from the suspended graphene layer.

The energy of the electrons also plays an important role [**?**]. Typically, the energy distribution of electrons in a material being bombarded by energetic x-rays or electrons is known to present a high and broad peak for energies below ~ 50 eV [**?**]. In fact, electron - electron scattering events lead to an electron cascade resulting in the accumulation of electrons within this energy range in the materials [**?**].

Interestingly, the relatively low energy secondary electrons ($\leq 10 - 20$ eV) involved in the scattering events are acknowledged as the main cause of sample damage [**?**], along with the Auger emission process directly involving valence electrons [**?**]. Damage occurs as a result of chemical bond breaking. Such events are likely to happen when the electron energy resonates with the energy difference between occupied and empty levels. For an oxide material, the typical metal-oxygen bond dissociation energy is around a few eV. The bond dissociation energy for the Ti-O bond in TiO_2 is $E_b^{Ti-O} \approx 6$ eV. Thus, low energy secondary electrons are the most likely to induce bond breaking and damage.

The general phenomena presented and discussed here for TiO_2 is not specific to this material. Quantitative differences are expected for different materials due to different damage mechanism and specific dose thresholds.

3.3 Effect of substrate thickness

Figure 2 presents spatially resolved XPS spectra obtained on an oxide film grown on multilayer ($\geq 5 - 10$ layers) graphene, as evidenced by Raman spectroscopy (see SI figure S1). In these samples, we observed damage of the TiO_2 film independent of the beam position. The spectral features are qualitatively very similar to the ones observed in Fig. 1 (a) and described above. This observation indicates that the number of secondary electrons causing damage may saturate when the substrate thickness becomes comparable to or larger than the inelastic mean free path ≈ 1 nm of the photo-generated electrons. This typical inelastic mean free path corresponds to approximately 3 graphene layers. This agrees with recent studies that show a rapid increase of secondary electron yield with an increasing number of graphene layers [**?**].

Here, considering the presence of ~ 10 graphene layers, we can estimate the substrate thickness over the suspended region as $D_S \approx 3$ nm, which is similar to the sample thickness. With a secondary electron yield close to that of graphite, a significant number of secondary electrons may originate from the substrate to induce damage in the oxide film.

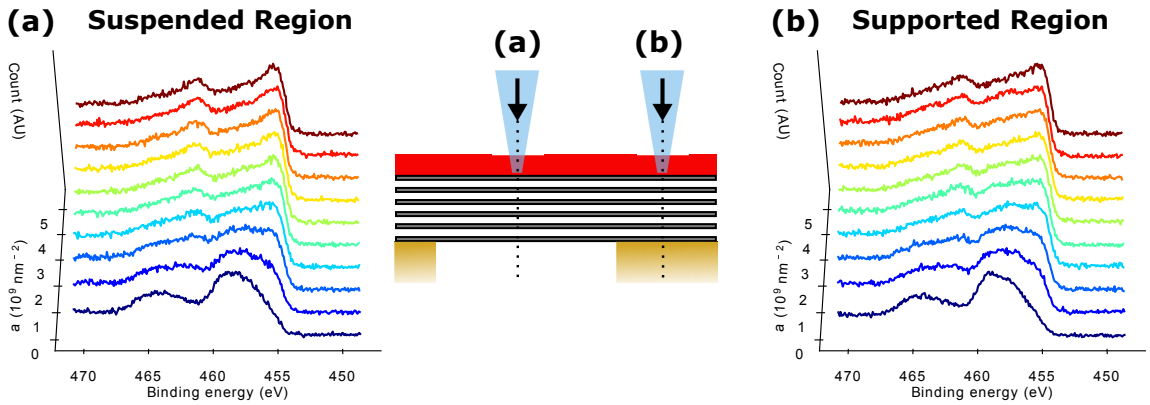

Figure 2: **Multilayer graphene** High resolution Ti 2p XPS spectra acquired over time on suspended (**a**) and supported (**b**) regions. The inset displays a schematic representation of the sample and the typical positions of the spatially resolved spectroscopy experiment corresponding to the two different situations.

This result provides further evidence for a damage mechanism in thin films resulting from secondary electrons generated in the substrate. It also emphasizes that: 1) an electron transparent suspending layer is critical to reduce damage, and 2) this damage limitation strategy will work for sample thicknesses on the order of the inelastic mean free path of electrons. Point 1) implies that adequate engineering of the substrate geometry can lead to directed patterning of the sample using a wide beam exposure.

3.4 Critical irradiation and damage rate

We now explore in more detail the dynamics of the damage mechanism taking place in the TiO_2 film.

As observed in Fig. 1 (b) and 2 (a)-(b), sample damage manifests as a shift towards lower binding energies reminiscent of a reduction of the initial Ti^{4+} due the ejection of oxygen atoms from the oxide film [**?**]. Quantitative contribution of the different oxidation states was determined by peak fitting. The XPS spectra are fitted using tabulated values for the different Ti oxidation state lineshapes (see Supplementary Information S3 for a complete description of the fitting procedure) [**?**, **?**]. In Figure 3 (a)-(b), and (d)-(e), we compare the spectra for the lowest and largest number of photons per unit area for a sample supported on single layer graphene and multilayer graphene, respectively. The corresponding contributions of the different oxidation states Ti^{4+} (red dotted line), Ti^{3+} (green dotted line) and Ti^{2+} (black dotted dashed line) to the total spectrum (red line) are displayed along with the experimental data

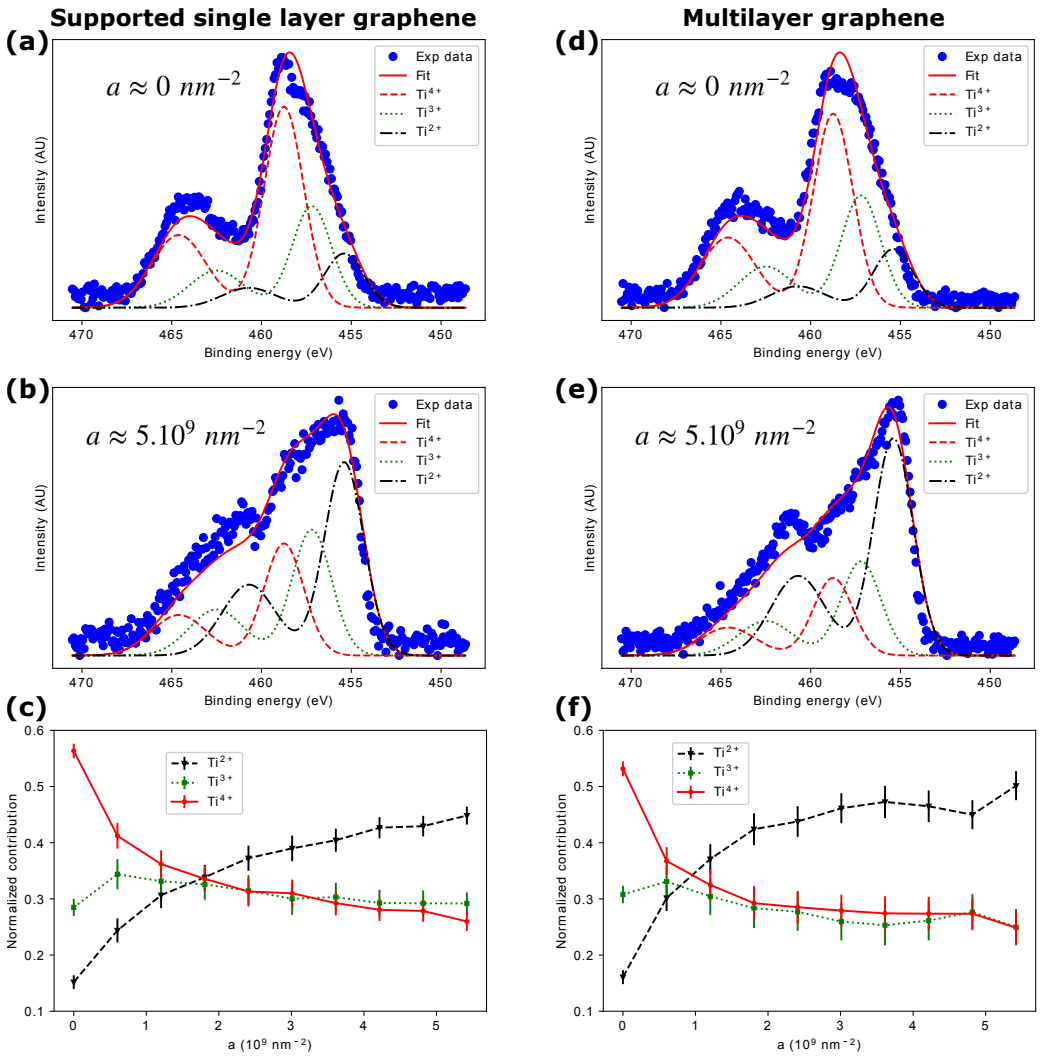

Figure 3: **Ti oxidation states and damage rate** Ti 2p XPS spectra at different number of photons per unit area for **(a)-(b)** a samples supported on single layer graphene and **(d)-(e)** a sample supported on multilayer graphene. The graphs display the different oxidation state contributions, Ti^{4+} (red dotted line), Ti^{3+} (green dotted line) and Ti^{2+} (black dotted dashed line), to the fit of the overall spectrum (red line) to the experimental data (blue dots). **(c)-(f)** Normalized contributions of the different oxidation states Ti^{4+} (red line), Ti^{3+} (green dotted line) and Ti^{2+} (black dashed line) as a function of the number of photons per unit area. The error bars represent the standard deviation error on the parameters obtained from the fit.

points (blue dots). First, we observe that the spectral features corresponding to these 3 different oxidation states combine well to accurately fit the experimental data. Then, we extract the evolution of the relative population of the different oxidation states as the sample irradiation increases (Fig. 3 (c)-(f)). The amount of Ti^{3+}

remains relatively constant whereas the contribution from Ti^{2+} increases significantly. Eventually, the distribution of oxidation states plateaus at a point where the amount of Ti^{4+} and Ti^{3+} are similar, slightly below 30%, and the amount of Ti^{2+} reaches $\approx 50\%$.

The evolution of the Ti oxidation state distribution with x-ray dose is qualitatively similar for the oxide film supported on single layer and multilayer graphene. However the multilayer graphene supported samples show a higher damage rate as evidenced by the earlier crossover point between the Ti^{4+} (red line) and Ti^{2+} (black dashed line) contributions in Fig. 3 (f). This effect could arise from an imperfect mechanical contact between the single layer graphene and the gold layer on the SiN support. Such imperfect contact may limit the transmission of secondary electrons from the gold layer to the graphene and eventually to the TiO_2 film.

4 Conclusion

We used thin oxide films as a model system to show that a significant contributor to radiation damage in thin films arises from secondary electrons generated in the substrate. We also demonstrate the benefit of using an ultra-thin suspended membrane, for example, graphene, as an x-ray transparent, metallic substrate for damage-free x-ray spectroscopy experiments. Quantifying the impact of radiation-induced damage is important to rule out any damage-related artifacts in high energy spectroscopy experiments. Furthermore, our results demonstrate a promising protocol to minimize radiation damage, offering a potential strategy for the development of specific beam sensitive sample holders. We also show that beam patterning can be achieved in thin films by designing the substrate with supported and suspended regions. Such technique could be of interest for high throughput film patterning that does not require beam rastering and positioning steps.

Acknowledgements

This work was supported by the U.S. Department of Energy, Office of Science, Office of Basic Energy Sciences, Materials Sciences and Engineering Division, under Contract No. DEAC02-05-CH11231 within the Inorganic/Organic Nanocomposites Program (KC3104). Part of the work was carried out as a user project at Molecular Foundry, supported by the Office of Science, Office of Basic Energy Sciences, of the U.S. Department of Energy under Contract No. DE-AC02-05CH11231.
We acknowledge the Elettra Synchrotron for the beamtime allocation, technical sup-

port and handling of the experiments.

Conflict of interest

The authors declare no competing interests.